TURBULENT REACTING MIXING OF LIQUIDS IN A COAXIAL JET MIXER

Matthias Walter, Nikolai Kornev
Institute for Modeling and Simulation
Faculty of Mechanical Engineering and Marine Technology
University of Rostock
Albert-Einstein-Str. 2, D-18059 Rostock, Germany
matthias.walter@uni-rostock.de

Egon Hassel
Institute for Technical Thermodynamics
Faculty of Mechanical Engineering and Marine Technology
University of Rostock
Albert-Einstein-Str. 2, D-18059 Rostock, Germany
egon.hassel@uni-rostock.de

ABSTRACT

Large eddy simulation is used to investigate passive and reactive scalar mixing at high Reynolds *Re* and Schmidt *Sc* numbers in order to prove capability of the LES-SGS micromixing approaches based on the eddy dissipation and DQMOM-IEM models properly simulating liquid reacting flows. Simulations were performed for a fast neutralisation reaction in a confined jet reactor. The mean profiles for passive scalar agree well with measurements. It was shown that the most contribution to the scalar variance is made by large scale motions whereas the contribution of fine scales smaller than typical inertial range scales is negligible. Thus, the existing LES models are capable of predicting the scalar variance at large *Sc* numbers. The results obtained for reactive transport revealed discrepancies in the determination of micromixing rate and product concentration. A special study was performed to investigate the dynamics of fine structures using locally refined box embedded into global grid. Typical statistical properties of fine structures were reproduced numerically.

INTRODUCTION

Mixing of passive or reactive substances within turbulent flow regimes occurs in many practical engineering applications such as reactors, heat exchangers or injection systems. Especially in the context of chemical engineering study of physical mechanisms of mixing processes is extremely important to control chemical reactions. The analysis and reproduction of the dynamics of fine scalar structures at high Schmidt $Sc \gg 1$ and Reynolds $Re \gg 1$ numbers belongs to the most complicated problems in fluid mechanics. In recent years small-scale structures in scalar mixing have already been thoroughly investigated by several authors using DNS (for instance Sreenivasan & Prasad (1989), Schumacher & Sreenivasan (2003), Schumacher *et al.* (2005), Yeung *et al.* (2004)). In spite of new fundamental insights into the physics of turbulent mixing at low and high Schmidt numbers gained recently, the modeling of mixing in liquids is still remaining a very challenging problem. The computer resources necessary to resolve the Batchelor scales $\eta_B = \eta\sqrt{Sc}$ at large Re numbers and small Kolmogorov scales η, exceed the capability of available modern super computers. For the full developed turbulent liquid flows, the scalar structures with scales of few Batchelor lengths become insomuch small compared to these of gas flows that a DNS is almost impracticable at least for the scalar dynamics. That is why the vast majority of numerical simulations published in the literature has been carried out for isotropic turbulence at low and moderate Reynolds numbers. So far, there are only few numerical results available considering turbulent scalar mixing at $Sc \gg 1$ and $Re \gg 1$.

In this work the reactive scalar mixing process is studied in a turbulent shear flow generated within a confined jet reactor, as shown in Figure 1. Computations are conducted using LES in order to overcome the high computational complexity emerging from DNS application. The coaxial jet mixer consists of a

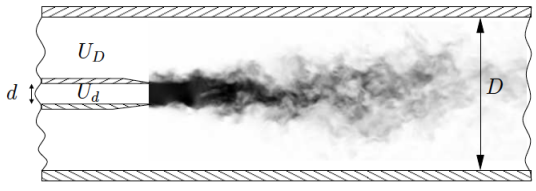

Figure 1. Sketch of the coaxial jet mixer along centerline.

nozzle of diameter $d = 0.01m$ positioned along the centerline of a pipe of diameter $D = 0.05m$ with the length $L = 0.6m$. From dimensional analysis it can be shown that the characteristics of the jet mixer depend for the isothermal case on the diameter ratio D/d, the Reynolds number related to the nozzle flow $Re_d = dU_d/\nu$, the Schmidt number Sc and the flow rate ratio $\dot{V}_D/\dot{V}_d$, whereas the jet velocity exceeds the coflow one. By variation of the diameter ratio or flow rate ratio two flow regimes can be observed. If $D/d < 1+\dot{V}_D/\dot{V}_d$ the flow is similar to a free jet. Otherwise if $D/d > 1+\dot{V}_D/\dot{V}_d$ a strong recirculation zone is created just behind the nozzle.

Despite efforts in the development of new scalar mixing approaches in the last years, there are only few suitable mixing models for LES considering the case $Sc \gg 1$. Mostly they are adopted and extented from RANS combustion modeling. The remaining challenge in LES modeling of liquid flows is an adequate reproduction of the influence of small-scale scalar structures in order to predict accurately mixing or reaction rates still at moderate mesh resolutions. In this paper, mixing at the subgrid level is modeled by DQMOM-IEM approach and common transport equation for mixture fraction using no further micromixing models. The aim of this study is to prove capability of these approaches properly simulating liquid reacting flows. Additionally within the simulations fine scalar structures up to few Batchelor scales have been carefully analysed with respect to selected statistical properties.

NUMERICAL METHOD

The governing equations for LES are derived by filtering the continuity equation, the Navier-Stokes equation and the advection-diffusion equation for the mixture fraction field $\phi(\mathbf{x},t)$ at the filter width $\overline{\Delta}$.

$$\frac{\partial \overline{u}_i}{\partial x_i} = 0, \tag{1}$$

$$\frac{\partial \overline{u}_i}{\partial t} + \frac{\partial \overline{u}_i \overline{u}_j}{\partial x_j} = -\frac{1}{\rho}\frac{\partial \overline{p}}{\partial x_i} + \frac{\partial}{\partial x_j}\left[\nu\left(\frac{\partial \overline{u}_i}{\partial x_j} + \frac{\partial \overline{u}_j}{\partial x_i}\right) - \tau_{ij}\right], \tag{2}$$

$$\frac{\partial \overline{\phi}}{\partial t} + \frac{\partial \overline{u}_j \overline{\phi}}{\partial x_j} = \frac{\partial}{\partial x_j}\left[D\frac{\partial \overline{\phi}}{\partial x_j} - J_j^{SGS}\right] \tag{3}$$

whereas the unclosed subgrid stress tensor

$$\tau_{ij} = \overline{u_i u_j} - \overline{u_i}\,\overline{u_j} \tag{4}$$

and the contribution to the subgrid scalar dynamics

$$J_j^{SGS} = \overline{\phi u_j} - \overline{\phi}\,\overline{u_j} \tag{5}$$

are modeled in terms of the filtered velocity $\overline{\mathbf{u}}$ and passive scalar $\overline{\phi}$. The subgrid stress tensor was closed first using a localized dynamic mixed model (Vreman *et al.* (1994)) adopted by a special clipping procedure based on the Taylor series approximation to avoid numerical instabilities (Kornev *et al.* (2006)). The LES results shown that the calculation of the internal SGS model coefficients without averaging in any homogeneous flow directions leads to high values in the dynamic calculation of the turbulent diffusion coefficents. The averaging is difficult to apply in flows without distinct homogenous direction or without a-priori knowledge about the flow regime like in the case under consideration. For this reason an extended lagrangian dynamic mixed model, developed by Meneveau *et al.* (1996), was subsequently used to close all SGS parts. The term J_j^{SGS} has been determined by the widley-used gradient diffusion approach whereas the neccessary turbulent diffusion coefficient D_t is dynamically computed from the lagrangian SGS model.

Reactive mixing modeling

As test reaction, a simple neutralisation of acid and base was investigated because well tried experimental data are available for validation purposes. Within this work two different simulations strategies are adopted for reactive mixing. The first simulation solves equation (3) with the subgrid dynamics directly modeled by SGS approaches. Therefore no additional micromixing model is needed. Instead of solving all species transport equations separately, a reaction progress variable $\overline{Y}$ was used to simplify the calculations,

$$\frac{\partial \overline{Y}}{\partial t} + \frac{\partial \overline{u}_j \overline{Y}}{\partial x_j} = \frac{\partial}{\partial x_j}\left[(D+D_t)\frac{\partial \overline{Y}}{\partial x_j}\right] + \overline{S(Y)} \tag{6}$$

where the filtered chemical source term $\overline{S(Y)}$ has to be modeled. Often the neutralisation reaction can be assumed as instantaneous compared to the characteristic mixing time scales and therefore $\overline{Y}$ can only be written in terms of mixture fraction $\overline{\phi}$,

$$\overline{Y}_\infty = min\left(\frac{\overline{\phi}}{\phi_{st}}, \frac{1-\overline{\phi}}{1-\phi_{st}}\right). \tag{7}$$

The expression (7) implies that both reagents cannot coexist at any point of the flow what may lead to errors in the prediction of product yield due to the unconsidered fluctuations of reagents. Another approach for the fast chemistry limit is a finite rate eddy dissipation model (EDM), which simply slows down the reaction rate whenever it is faster than the micromixing rate. According to Fox (2003), the EDM can be written as

$$\overline{S(Y)} = min\left(S(\overline{Y}), C\frac{\overline{\varepsilon_\phi^{SGS}}}{\overline{\phi_{SGS}^{\prime 2}}}\right) \tag{8}$$

whereas the timescale of fluid dynamic dissipation k/ε is replaced by the time scale of scalar dissipation $\overline{\phi_{SGS}^{\prime 2}}/\overline{\varepsilon_\phi^{SGS}}$ to account for high Schmidt number effects. The SGS dissipation rate $\overline{\varepsilon_\phi^{SGS}}$ and SGS scalar variance $\overline{\phi_{SGS}^{\prime 2}}$ require further modeling. The constant C is determined empirically and the

term $S(\overline{Y})$ is calculated using following expression,

$$S(\overline{Y}) = \phi_{st} r B_0 \left(\frac{1-\overline{\phi}}{1-\phi_{st}} - \overline{Y} \right) \left(\frac{\overline{\phi}}{\phi_{st}} - \overline{Y} \right) \tag{9}$$

where r is the reaction rate constant, C_{B0} is the inital concentration of reagent B and ϕ_{st} is the stoichiometric mixture fraction with $\phi_{st} = C_{A0}/(C_{A0}+C_{B0})$. The unknown concentration values can be calculated from simple algebraic relations using the reaction progress variable and the mixture fraction (Fox (2003)).
The SGS scalar variance $\overline{\phi'^2_{SGS}}$ is modeled in terms of scale similarity model

$$\overline{\phi'^2_{SGS}} = Cs \left(\widetilde{\overline{\phi}\,\overline{\phi}} - \tilde{\overline{\phi}}\,\tilde{\overline{\phi}} \right) \tag{10}$$

and the SGS scalar dissipation rate $\overline{\varepsilon_\phi^{SGS}}$ is computed using a simple linear relaxation model

$$\overline{\varepsilon_\phi^{SGS}} = 2C_x \frac{D_t \phi}{\Delta 2} \overline{\phi'^2} = 2C_x |\overline{S}| \overline{\phi'^2_{SGS}}, \tag{11}$$

where C_x is dynamically determined by the SGS model.
The second simulation was carried out using DQMOM in association with the Interaction by Exchange with the Mean (IEM) mixing model. This approach is based on the assumption that the transport of the joint composition PDF $\overline{P}_\theta(\psi, \mathbf{x}, t)$

$$\frac{\partial \overline{P}_\theta}{\partial t} + \frac{\partial \overline{u}_j \overline{P}_\theta}{\partial x_j} = \frac{\partial}{\partial x_j} \left[(D + D_t) \frac{\partial \overline{P}_\theta}{\partial x_j} \right] - \frac{\partial}{\partial \psi} \left[\frac{1}{\tau} (\overline{\theta} - \psi) \overline{P}_\theta \right] \tag{12}$$

can be approximated by finite number of moments through a summation of N_e Dirac delta peaks (Fox (2003), Raman *et al.* (2005))

$$\overline{P}_\theta(\psi, \mathbf{x}, t) = \sum_{n=1}^{N_e} \overline{p}_n(\mathbf{x}, t) \prod_{\alpha=1}^{N_s} \delta(\psi - \overline{\theta}_{\alpha n}(\mathbf{x}, t)), \tag{13}$$

whereas N_s is the number of species, $\overline{\theta}_{\alpha n}$ depicts the location of delta peaks in composition space and $\overline{p}_n$ is the filtered volume fraction of the n-th environment. Substituting (13) into (12), transport equations for $\overline{p}_n$ and $\overline{p_n \theta}_n$ are given as

$$\frac{\partial \overline{p}_n}{\partial t} + \frac{\partial \overline{u}_j \overline{p}_n}{\partial x_j} = \frac{\partial}{\partial x_j} \left[(D + D_t) \frac{\partial \overline{p}_n}{\partial x_j} \right] + a_n \tag{14}$$

$$\frac{\partial \overline{p_n \theta_n}}{\partial t} + \frac{\partial \overline{u}_j \overline{p_n \theta_n}}{\partial x_j} = \frac{\partial}{\partial x_j} \left[(D + D_t) \frac{\partial \overline{p_n \theta_n}}{\partial x_j} \right] + b_{\alpha n}. \tag{15}$$

In order to ensure the realizability of the PDF associated with IEM model the source terms a_n for transport equation of the volume fraction are set to zero (Fox (2003)). The remaining source terms $b_{\alpha n}$ are determined by moments of the transport term in composition space using the DQMOM method. Details of this method as well as the derivation of the source terms can be obtained from the original papers of Fox (2003) and Marchisio & Fox (2005). Global continuity requires that the volume fractions sum up to one

$$\sum_{n=1}^{N} p_n = 1. \tag{16}$$

The local filtered value of $\overline{\theta}_n$ in environment n can be expressed as

$$\overline{\theta}_n = \frac{\overline{p_n \theta_n}}{p_n}, \tag{17}$$

whereas the filtered value of $\overline{\theta}$ is defined by

$$\overline{\theta} = \sum_{n=1}^{N} \overline{p_n \theta_n} \tag{18}$$

and subsequently, the variance of $\overline{\theta}$ can be expressed by

$$\overline{\theta'^2} = \sum_{n=1}^{N} p_n (\overline{\theta}_n - \overline{\theta})^2. \tag{19}$$

In this work three environments have been used two of them represent the inlet streams and one the reaction zone. The total number of transport equations for the chemical system under consideration is five. Since the neutralisation reaction can be assumed as infinitely fast and to avoid numerical instabilities due to the high reaction rate associated with a finite-rate chemistry solver, the reaction progress variable $\overline{Y}$ is calculated by equation (7) whereas the value of the mixture fraction $\overline{\phi}$ is calculated by solving the appropriate transport equations for $\overline{p}_1$, $\overline{p}_2$, $\overline{p_1 \phi_1}$,$\overline{p_2 \phi_2}$ and $\overline{p_3 \phi_3}$. Note that the correction term $b_{\alpha n}$ in eq. (15) includes a micromixing parameter $\gamma = C_\phi/\tau$ responsible for the destruction of subgrid-scale scalar gradients. The choice of γ is strongly coupled to problem under investigation and cannot be determined universally . Using the formulation of Colucci *et al.* (1998) , the turbulence time scale can be determined as $\tau = 2\Delta^2/(D + D_t)$ whereas the scalar-to-mechanical ratio C_ϕ has to be chosen depending on the flow regime in association with the type of reaction kinetics. In RANS simulations this quantity is usually calculated as a function of Schmidt number and local turbulent Reynolds number. In LES, however, the same approach cannot be used since it also depends on the unresolved fraction of turbulent and scalar spectrum (Marchisio (2009)). Sine in literature there are different data for C_ϕ, a sensitivity analysis has been done in this work to find out a proper value for C_ϕ matching the available experimental data at best.

NUMERICAL SETUP

Simulations have been performed using OpenFOAM® which is based on a 3-D finite volume method for arbitrary non orthogonal grids. The discretisation in space and time

of the transported and transporting quantities at the cell faces is of second order using a central differencing scheme. For the simulations of reactive and passive scalar transport conducted in this study the ratio of volumetric rates of the coflow to the jet was equal $\dot{V}_D/\dot{V}_d = 5$. The equations are solved on a cartesian O-grid with 1.3 Mio cells refined near the mixer axis and nozzle exit. Grid independence was already guaranteed by previous simulations published by the authors. No slip boundary conditions were applied on the pipe walls and zero gradient condition at the outlet. LES inlet conditions were initialised using auxiliary precusor calculations of a quasi periodic pipe flow providing fluctuations and mean velocity at the inlet of the actual computational domain. Coflow inlet velocity profile ($U_{Dbulk} = 0.228m/s$) was obtained from experiments. The simulations were carried out for the jet exit velocity of $U_{d\,max} = 1.58m/s$ ($U_{d\,bulk} = 1.192m/s$) corresponding to the Reynolds number of $Re_d = 10500$. According to the definition of the mixture fraction, $\overline{\phi}$ is equal to one at jet exit and to zero at coflow entrance whereas the scalar variance $\overline{\phi'^2}$ equals zero in both sections. The Schmidt number was $Sc = 1000$ whereas the turbulent part Sc_t was dynamically determined within the SGS model using an eddy diffusivity approach. The inital concentrations of reagents HCL and $NaOH$ are $C_{HCL} = 1.2mol/m^3$ and $C_{NaOH} = 18mol/m^3$. Assuming an isothermal reaction the Arrhenius equation can be simplified to one reaction rate constant $r = 10^8 m^3/mol\,s$.

Examination of small-scale statistics

From previous work of Kornev *et al.* (2008) the Kolmogorov scale was estimated lying within a range of $\eta = 31..300\mu m$ what corresponds to the range of Batchelor scale η_B between 1 and $10\mu m$. Since it was impossible to resolve the complete domain up to η_B or even up to η we introduce a small box of 2x1x1 mm centered at $x/D = 0.4$, $r/D = 0.06$ with a very high resolution of $\sim 4\mu m$ as shown in Figure 2. In order to avoid numerical instabilities related to the pressure correction method and for a smooth transport of small-scale structures coming from LES area to region of interest, the mesh refinement has been done smoothly from coarse resolution far from the box to the finest one inside the box. It is assumed that the flow structures moving downstream within refining grid become small and enter the high resolved box where they have opportunity to be transformed into the structures with nearly Kolmogorov or even Batchelor scales. It is supposed that the statistical properties of the fine scale turbulence will be reproduced properly by structures developing within such a box. This way is similar to that where a small box of turbulence is studied using periodic boundary conditions with forcing to maintain a certain level of turbulent fluctuations. An advantage of the presented method is the possibility to maintain the turbulence by a natural way and to study the influence of large scale effects (gradients of the velocity and mixture fraction) on the fine structure dynamics. In these simulation the time step Δt was set to $10^{-7}s$.

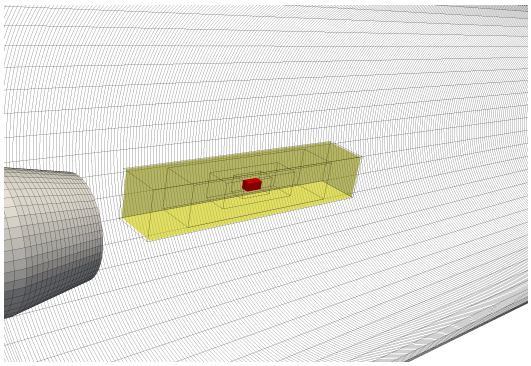

Figure 2. The area of refinement (yellow) consists of 192 Mio cells. The grid resolution of the highest refinement level (red) is about $4\mu m$ at $\sim$ 78Mio cells.

RESULTS

Figure 3 shows the profile of time-averaged mixture fraction obtained from LES and experiment along the x-axis at the centerline of the domain. As seen $\overline{\phi}$ remains constant in the initial jet region at $0 < x/D < 0.5$ containing only HCL. The chemical reaction takes place on the boundary between jet and coflow. At $x/D > 0.5$ the jet breaks up due to forming vortices on the jet boundary caused by the natural instability of the shear layer. The mixing arrives the jet centerline and it is completed at $x/D > 7$ with the formation of a homogenous mixture. Both LES predictions for the averaged mixture fraction agree well with experimental data.

Figure 4 demonstrates the profile of the time-averaged r.m.s

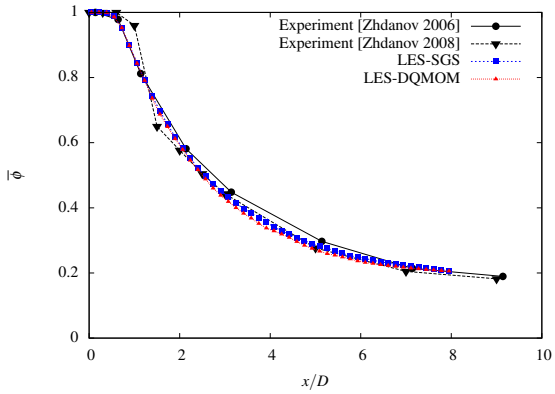

Figure 3. Time-averaged mixture fraction along main flow direction at the centerline of the jet mixer.

values of $\overline{\phi}$ along the centerline of the jet mixer. As seen, LES prediction with directly modeled subgrid dynamics shows only small discrepancies compared to measurements whereas DQMOM model overpredicts $\overline{\phi'}$ more than three times. The reason for the difference can be traced back to numerical instabilities in the treatment of spurious dissipation term in the correction term $b_{\alpha n}$ of eq. (15) which is directly responsible for the variance of the PDF as well as for all higher moments. Investigations by Fox et al. revealed that singularities in $b_{\alpha n}$ occur if the distance between delta peaks in composition space falls below a certain limit. Wang & Fox (2004) proposed a

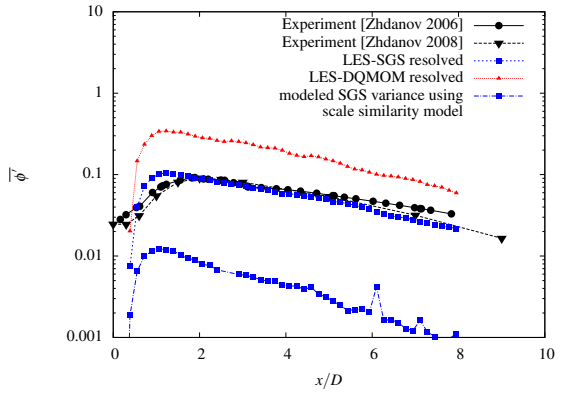

Figure 4. Time-averaged r.m.s. values of mixture fraction along main flow direction at the centerline of the jet mixer.

method to control the realizability by bounding $\overline{\phi}_n$ to its theoretically limit less some small positive number ε. Every time $\overline{\phi}_n$ lies ouside of $[\varepsilon, 1-\varepsilon]$ the correction term $b_{\alpha n}$ will be set to zero. Although the presented method has been applied for realizability control in the simulations the second moment of $\overline{\phi}$ still differs significantly from experiment and LES using only subgrid dynamics. Therefore the issue of realizability control associated with proper initial conditions for $\overline{\phi}_n$ and $\overline{p_n \phi_n}$ will be object of investigation in the next stage. However, despite the shortcomings of DQMOM-IEM in variance modeling both LES mixing approaches provide good results for the mean mixture fraction $\overline{\phi}$ at $Sc = 1000$ since the main contribution to scalar variance is caused by large scale motions. The contributions from oscillations within a few Batchelor lengths, which were not taken into account in the LES models as well as the contributions of the unresolved scales determined by the scale similarity model as shown in Figure 4, are of minor importance.

Figure 5 shows the mean concentration of the reaction product along the centerline of the jet mixer. The LES results

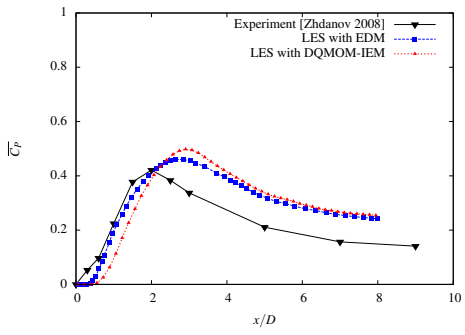

Figure 5. Distribution of mean product concentration along main flow direction at the centerline of the jet mixer.

are compared with experimental data obtained using PLIF and titration method. The chemical reaction along the centerline starts to proceed in the region where the mixing caused by the strong vortices in the mixing layer arrives the centerline and the mixture fraction becomes less than one. The analysis of experimental data revealed a relatively large discrepancy between the product directly measured and the product calculated using the instantaneous mixture fraction at resolution of $300\mu m$. It means that the micromixing effects are not negligible and can be essential although the reaction is very fast. The reason for the discrepancy between simulations and measurements are drawbacks of the micromixing models. Both EDM and DQMOM-IEM involve a constant fitted to match the target distribution of product concentration from measurements. Despite fitting both models still overestimate the micromixing rate resulting in a discrepancy of $\sim 10\%$ for product concentration compared to experiment. Additionally the point of the highest product conversion is displaced from $x/D = 2$ to $x/D = 3$. Another reason for discrepancy with measurement and DQMOM-IEM model is the problematic numerical treatment of spurious dissipation term that also affects the micromixing rate. Furthermore the number of environments used in the DQMOM-IEM model can possibly be insufficient to represent properly the reactive scalar transport for the initial concentration ratio used in this work.

Micromixing

As seen in the spatial spectrum of scalar fluctuations (Figure 6) the inertial convective range of the spectrum is well reproduced. Although the Batchelor scale is not completely resolved by the mesh the viscous-convective subrange of the scalar spectrum possess a trend towards the k^{-1} scaling predicted by Batchelor and Kraichnan. This result is in a good agreement with the scalar spectrum obtained from PLIF measurements of Kornev *et al.* (2008). However it should be noted that only a small part of the viscous-convective subrange of the scalar spectrum could be captured since size and resolution of the region of interest was restricted by available computer power. The presence of areas with rapid change in the

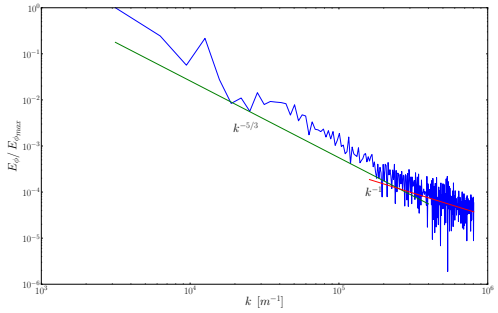

Figure 6. Scalar spectrum at $x/D = 0.4$, obtained by probes in main flow direction.

scalar shown in Figure 7 is characteristic for turbulent mixing of liquids. The resulting cliff-like structures presented in Figure 8 are responsible for small-scale intermittency (Warhaft (2000)). Figure 7 also confirms that the transition of scalar structures from coarse grid to region of interest (high resolved box) conveys information about small and large scale structures quite properly. The increase of the kurtosis of the struc-

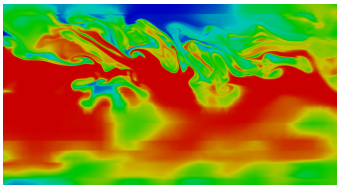

Figure 7. Snapshot of the instantaneous scalar field within the region of interest. As seen, the structures develop smoothly from coarse resolution to finest one inside the box.

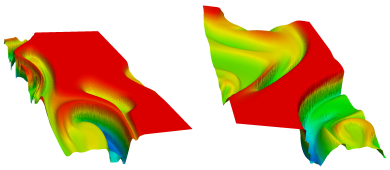

Figure 8. Forming fine scalar structures in turbulent mixing layer.

ture function of the first order $\Delta f(r) = f(x+r) - f(x)$ at $r \to 0$ points out that the scalar turbulence is non Gaussian (Figure 9). This suggests, that intermittency is observed both at the end of the inertial convective and the viscous-convective subranges. The Kurtosis converges to a Gaussian value of three at large separations r what coincides with results based on measurements from Kornev *et al.* (2008). A more detailed iden-

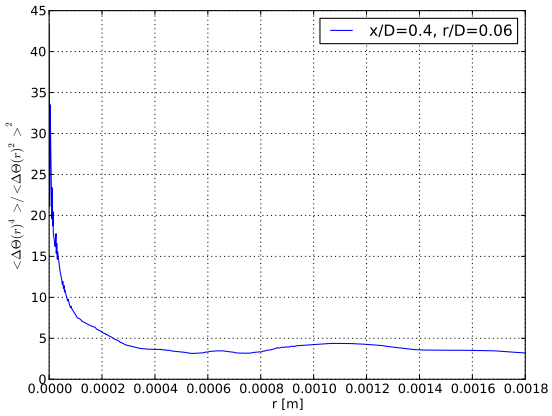

Figure 9. Kurtosis of the scalar difference $\Delta f(r) = f(x+r) - f(x)$ as a function of r.

tification of small-scale structures can be done analysing the 3D scalar dissipation rate $\chi = D\nabla\phi\nabla\phi$. The scalar dissipation rate is concentrated in thin sheet-like dissipation layers (Figure 10) substantially affecting the molecular diffusion process in the flow. Three basic topologies, first presented by Buch & Dahm (1996) and later experimentally confirmed by Kornev *et al.* (2008), were observed in the scalar field. They include long regions consisting of many straight and nearly parallel dissipation layers, areas where two such long regions meet orthogonally and spiral structures, as shown in Figure 11.

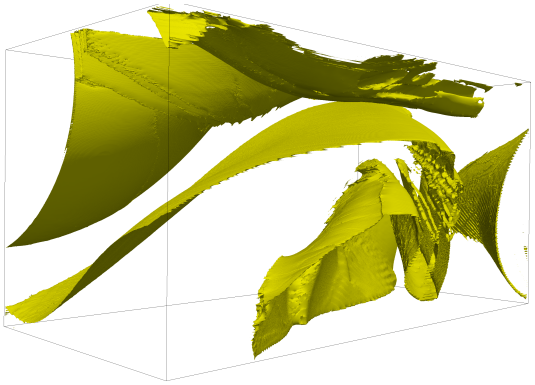

Figure 10. Isosurfaces of scalar dissipation rate visualized within the region of interest of size $2x1x1$mm. In contrast to gas-phase the small-scale structures in liquids evolve to extremely thin sheet-like strained laminar diffusion layers.

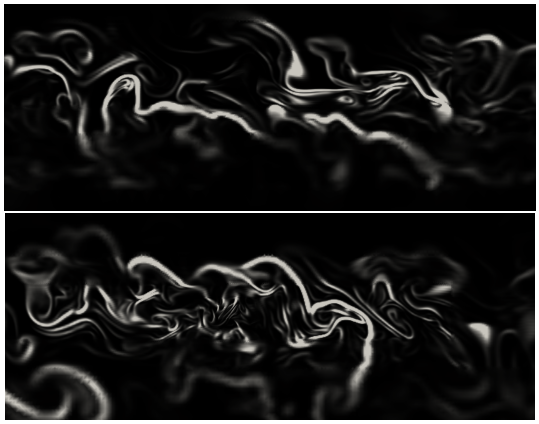

Figure 11. 2D snapshots of scalar dissipation rate indicating three regular structures within the scalar field. The window size is $2x1$mm.

CONCLUSION

A comparative numerical study of LES micromixing models for passive and reactive scalar transport at high Reynolds and Schmidt number was performed. Two LES-SGS micromixing approaches based on the eddy dissipation and DQMOM-IEM models were applied to study the fast neutralisation reaction of acid and base in a confined jet reactor with very diluted inlet concentrations. Within the DQMOM-IEM approach the spurious dissipation term responsible for determination of higher moments was specially treated to avoid singularities.

Both micromixing models reproduce the mean distribution of the passive scalar accurately. The passive scalar variance obtained using scale similarity model agrees well with measurements whereas the DQMOM model shows large discrepancy.

However, this fact does not mean that the micromixing is described properly using the time scale of scalar dissipation at high Sc numbers within the calculation of the micromixing rate. The scalar variance for the case under consideration is dominated by large scale fluctuations which can be captured by existing LES models even developed for the $Sc \sim 1$ case. Deficits of both models become apparent in validation study for product concentration. The micromixing rate is overestimated by both mixing approaches resulting downstream in a higher product concentration compared with experimental data. A special study was performed to investigate the fine structures dynamics. For that the grid was locally refined up to scales comparable with Batchelor ones. The spectrum of scalar fluctuations shows the tendency to the k^{-1} scaling law predicted by Batchelor and Kraichnan for $Re >> 1$ and $Sc >> 1$. Three basic topologies previously predicted by Dahm et al. can be identified in the scalar field. They include long regions consisting of many straight and nearly parallel dissipation layers, areas where two such long regions meet orthogonally and spiral structures. Small scale intermittency caused by cliff-like structures in the scalar field was proven to exist up to Batchelor scales. Furthermore it was shown that the dissipation is localised in thin sheet-like strained laminar-diffusion layers between adjacent interacting layers of different mediums.

ACKNOWLEDGEMENTS

Numerical simulations have been performed using the resources of the North German Supercomputing Alliance (HLRN).

REFERENCES

Buch, K.A. & Dahm, W.J.A. 1996 Experimental study of the fine-scale structure of conserved scalar mixing in turbulent shear flows, part i: $sc >> 1$. *J. Fluid Mech.* **317**, 21–71.

Colucci, P.J., Jaberi, F.A. & Givi, P. 1998 Filtered density function for large eddy simulation of turbulent reacting flows. *Physics of Fluids* **10**, 499–515.

Fox, R. 2003 *Computational Models for Turbulent Reacting Flows.*. Cambridge University Press.

Kornev, N., Tkatchenko, I., & Hassel, E. 2006 A simple clipping procedure for the dynamic mixed model based on taylor series approximation. *Commun. Numer. Meth. Engng.* pp. 55–61.

Kornev, N., Zhdanov, V. & Hassel, E. 2008 Study of scalar macro- and microstructures in a confined jet. *Int. Journal Heat and Fluid Flow* **29** (3), 665–674.

Marchisio, D.L. 2009 Large eddy simulation of mixing and reaction in a confined impinging jets reactor. *Computers and Chemical Engineering* **33**, 408–420.

Marchisio, D.L. & Fox, R.O. 2005 Solution of population balanced equations using the direct quadrature method of moments. *Journal of Aerosol Science* **36** (1), 43–75.

Meneveau, C., Lund, T. & Cabot, W.H. 1996 A lagrangian dynamic subgrid-scale model of turbulence. *J. Fluid Mech.* **319**, 353–385.

Raman, V., Pitsch, H. & Fox, R.O. 2005 Eulerian transported probability density function sub-filter model for large eddy simualtions of turbulent combustion. *Combustion Theory and Modelling* **10**, 439–458.

Schumacher, J. & Sreenivasan, K.R. 2003 Geometric features of the mixing of passive scalars at high schmidt numbers. *Phys. Rev. Lett* **91**.

Schumacher, J., Sreenivasan, K.R. & Yeung, P.K. 2005 Very fine structures in scalar mixing. *J. Fluid Mech.* **513**.

Sreenivasan, K.R. & Prasad, R.R. 1989 New results on the fractal and multifractal structure of the large schmidt number passive scalars in fully turbulent flows. *Physica D* **38**, 322–329.

Vreman, B., Geurts, B. & Kuerten, H. 1994 On the formulation of the dynamic mixed subgrid-scale model. *Phys. Fluids* **6**, 4057–4059.

Wang, L. & Fox, R.O. 2004 Comparison of micromixing models for cfd simulation of nanoparticle formation. *AIChE Journal* **50** (9), 2217–2232.

Warhaft, Z. 2000 Passive scalars in tubulent flows. *Annu. Rev. Fluid Mech.* **32**, 203–240.

Yeung, P.K., Xu, S., Donzis, D.A. & Sreenivasan, K.R. 2004 Simulations of three-dimensional turbulent mixing for schmidt numbers of the order 1000. *Flow, Turbulence and Combustion* **72**, 333–347.